

Twisted Bi-Layer Graphene: Microscopic Rainbows

J. Campos-Delgado, G. Algara-Siller, C. N. Santos, U. Kaiser, and J.-P. Raskin*

Twisted bi-layer graphene (tBLG) has recently attracted interest due to the peculiar electrical properties that arise from its random rotational configurations. Our experiments on CVD-grown graphene from Cu foil and transferred onto Si substrates, with an oxide layer of 100 nm, reveal naturally-produced bi-layer graphene patches which present different colorations when shined with white light. In particular yellow-, pink- and blue- colored areas are evidenced. Combining optical microscopy, Raman spectroscopy and transmission electron microscopy we have been able to assign these colorations to ranges of rotational angles between the two graphene layers. Optical contrast simulations have been carried out, proving that the observation of the different colorations is due to the angle-dependent electronic properties of tBLG combined with the reflection that results from the layered structure tBLG/100 nm-thick SiO₂/Si. Our results could lead the way to an easy selective identification of bi-layer graphene merely through the observation on an optical microscope.

Carbon atoms covalently bonded and arranged in a honeycomb lattice constitute graphene. When two of these layers are stacked on top of each other a new material takes the scene, namely bi-layer graphene. Although bi-layer and multi-layer graphene have been studied along with single-layer graphene since its observation in 2004,^[1] the early reports consisted on mechanically exfoliated bi-layer, which maintained the AB stacking of HOPG.^[2,3] AB stacking or Bernal stacking is considered as the most stable way to arrange graphene layers in the Z-direction. This configuration is obtained by overlapping two graphene sheets in such a way that a carbon atom in one layer would sit on the center of the hexagonal ring from the other layer, corresponding to a rotational angle of 60°. However, when two graphene layers are randomly placed on top of each other, the overlap can generate a new superlattice in the form of a Moiré pattern. Different twist angles between the layers

will generate different Moiré patterns which can be visualized using high resolution transmission electron microscopy (HRTEM)^[4] or scanning tunneling microscopy (STM).^[5,6] In particular, Raman spectroscopy plays a very important role in identifying the stacking nature of graphene. In 2006, Ferrari and co-authors^[2] demonstrated that bi- and few- layer graphene derived from HOPG by mechanical exfoliation have a unique Raman fingerprint. It was later that scientists realized that artificially produced, chemical vapor deposition (CVD) grown and epitaxially grown bi-layer graphene samples had different stacking orders and hence different Raman spectra.^[7–11] It has been proven that the Moiré superlattices give rise to periodic potentials that alter the electronic dispersion of the structure. According to recent publications the extent to which the electronic properties are modified depends on the twist angle. For large angles the layers are decoupled and behave like single layer graphene ($\theta > 15^\circ$), which is the case for few-layer graphene grown on SiC.^[12] For intermediate angles ($2^\circ < \theta < 15^\circ$) the band velocity is decreased and van Hove singularities appear in the density of states (DOS), where the energy gap varies as a function of θ . For very small angles ($\theta < 2^\circ$) the Fermi velocity becomes angle dependent and sharp peaks appear close to the Dirac point.^[13,14] These van Hove singularities have been predicted theoretically and observed experimentally through scanning tunneling spectroscopy (STS)^[15–18] and angle-resolved photoemission spectroscopy (ARPES).^[19]

The optical properties of single layer graphene, Bernal-stacked and twisted bi-layer graphene are governed by their electronic structure. While single layer and Bernal-stacked bi-layer graphene show a constant absorption in the visible range (~2.3% and ~4.6%, respectively),^[20] for tBLG, the many van Hove singularities that appear in the DOS will alter accordingly the light absorption behavior for each rotational angle.^[21]

Producing artificial bi-layer graphene consists on intentionally placing two layers of graphene on top of each other, for instance by mechanically folding graphene^[22,23] or by transferring two CVD single-layer graphene sheets on a target substrate.^[24] Carozo and co-workers^[23] showed that by dragging graphene with an AFM tip it can be folded onto itself, artificially producing bi-layer graphene with well defined rotational angles. They reported on the superlattices thus formed and the appearance of new Raman spectroscopy features in the vicinity of the G-band, dependent on the angle of rotation, namely R and R' bands. Kim and co-workers^[24] artificially produced it by superimposing two CVD-grown graphene layers. Since CVD-grown graphene has a polycrystalline nature, they were able to produce bi-layer graphene

Dr. J. Campos-Delgado, Prof. J.-P. Raskin
ICTEAM, Université catholique de Louvain
Louvain-la-Neuve, 1348, Belgium
E-mail: jessica.campos@uclouvain.be

G. Algara-Siller, Prof. U. Kaiser
Ulm University
Group of electron microscopy for materials science
Ulm, 89081, Germany

Dr. C. N. Santos
IMCN/NAPS, Université catholique de Louvain
Louvain-la-Neuve, 1348, Belgium

DOI: 10.1002/sml.201300050



with a wide variety of rotational angles within the same sample. Coupling transmission electron microscopy (TEM) studies and Raman spectroscopy they showed striking differences in the electronic structure of twisted bi-layer graphene (tBLG).

The chemical vapor deposition of large area graphene using metals as catalysts produces mono-layer graphene and, inevitably, bi-layer patches.^[8–10] It has been proven that these bi-layer patches present differences in rotational angles due to the polycrystalline nature of the grown graphene.^[25–27] Havener and co-authors^[27] showed, using dark-field transmission electron microscopy and Raman spectroscopy, that areas of bi-layer CVD-grown graphene can be composed of domains with different rotational angles. They demonstrated an angle-dependent resonance of the G-band and showed that this resonance is also energy-dependent by probing the sample with different laser excitation energies. The above mentioned studies^[22–24,27] demonstrate that Raman spectroscopy constitutes a mighty tool to probe the angles of rotation in tBLG.

In this work we prove that bi-layer graphene produced by low pressure CVD transferred to SiO₂/Si substrates with a 100 nm oxide layer, shows differences in the optical reflection when observed with an optical microscope. Using Raman spectroscopy we have been able to find G-band resonances in these regions, which indicate that the color differences are directly related to the rotational angles between layers. This conclusion was further confirmed with TEM studies, and supported by simulations of the optical reflectance contrast for different θ values of tBLG.

The inspection of our samples by optical microscopy revealed peculiar colorations in the two layer patches that naturally appear in CVD-grown graphene. **Figure 1** shows micrographs of our samples where different colorations are visible in particular zones of the bi-layer graphene islands. Although the colorations can be observed without any treatment of the images, for the sake of clarity we have enhanced the contrast using software tools to render them more obvious (untreated images can be found in Figure S1 of the Supporting Information).

Our investigations reveal that the thickness of the silicon oxide layer is of paramount importance for the observation of these colorations. Besides our observations on Si

substrates with oxide thicknesses of 100 nm, we have transferred our samples to Si substrates with oxide thicknesses of 300 nm and 90 nm. For the 300 nm SiO₂ thickness, no colorations were found, not even after software treatment of the images. Subtle increases in contrast were found for some regions of the bi-layer patches where the G-band turned out to be resonant with $E_{\text{laser}} = 2.41$ eV ($\lambda = 514$ nm, Figure S2 C and D), as previously discussed in Reference [27]. Optical micrographs and Raman spectra of samples transferred to Si substrates with 300 nm oxide layer can be found in Figure S2 of the Supporting Information. In the case of 90 nm, pink colorations are the most evident and yellow- and blue-colored areas can be also identified but show a decrease in contrast (results not included here).

Although the differences in absorption properties are intrinsic to tBLGs dictated by their unique angle-dependent DOS, the colorations are not observed unless the optimal SiO₂ thickness is used. The observation of the different colorations is due to the angle-dependent electronic properties of tBLG combined with the reflection that results from the layered structure tBLG/100 nm-thick SiO₂/Si.

The reflectance of single- and multi-layer graphene on SiO₂ substrates has been widely studied^[20,28,29] however, to the best of our knowledge, this is the first time that different colorations are observed in bi-layer graphene. The colorations observed can mainly be catalogued as yellowish, bluish, and pinkish. We have performed a large number of Raman spectroscopy measurements of these particular areas using three different laser excitation energies. **Figure 2A** shows a representative micrograph of our samples where the above mentioned areas (yellow, blue, pink) are observed. Numbers 1, 2 and 3 point out the spots where measurements were recorded. Our measurements reveal that yellow areas show a strong G-band resonance with $E_{\text{laser}} = 2.54$ eV ($\lambda = 488$ nm, spot 1 in Figure 2A), blue areas show a G-band resonance when probed with $E_{\text{laser}} = 1.96$ eV ($\lambda = 633$ nm, spot 2 in Figure 2A) and for pink areas the G-band resonance is found with both, $E_{\text{laser}} = 2.41$ eV ($\lambda = 514$ nm) and $E_{\text{laser}} = 2.54$ eV ($\lambda = 488$ nm) (spot 3 in Figure 2A).

We have checked these color-dependent and energy-dependent resonances of the G-band at a larger scale by recording Raman maps. Figure 2B illustrates the area where maps were acquired, the image to the right corresponds to the

same image after software treatment, where zones of interest with pink, yellow and blue colorations are visible. The corresponding G-band intensity Raman maps are shown below the optical images, contours of the bi-layer areas have been included as guides to the eye. A careful cross-inspection of optical images and Raman maps reveals that pink and yellowish areas show the highest intensities when using $E_{\text{laser}} = 2.41$ eV ($\lambda = 514$ nm) and that the intensity is enhanced in bluish areas when using $E_{\text{laser}} = 1.96$ eV ($\lambda = 633$ nm).

To investigate the structural nature of these particularly-colored patches, we have performed TEM experiments. A

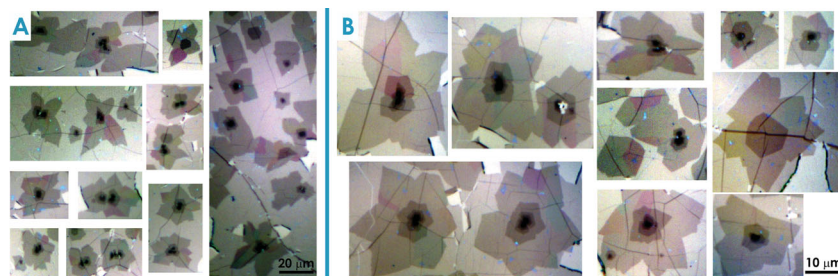


Figure 1. Optical micrographs of CVD-grown twisted bi-layer graphene transferred onto SiO₂/Si (oxide thickness 100 nm). A) and B) are images recorded with 50× and 100× objectives, respectively. Images have been treated with software to enhance the levels of contrast and to make more evident the differences in optical reflection. Sharp blue dots correspond to PMMA residues from the transfer process. Unmodified original frames are included in the Supporting Information as Figure S1.

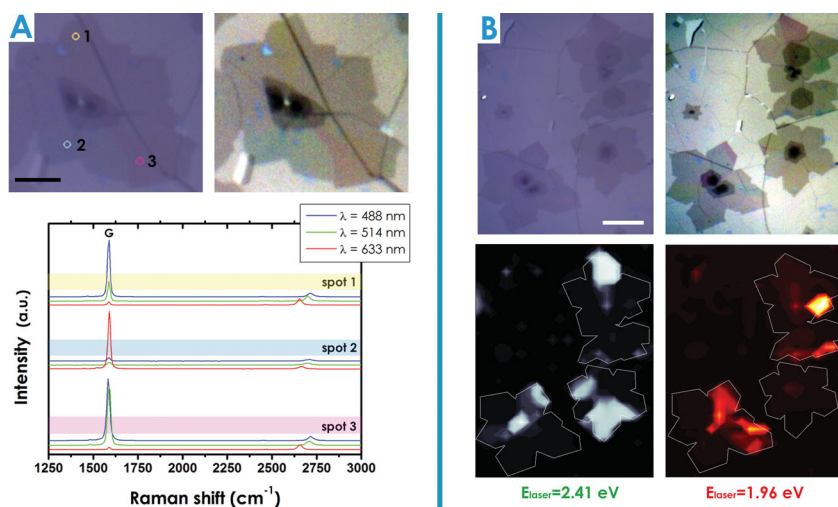


Figure 2. A) Optical image of sample on SiO₂/Si (SiO₂ = 100 nm) and, to the right, the same image treated with software to enhance visibility of different regions. Scale bar = 5 μm. Spots marked with circles and numbers (1, 2, 3) specify areas where single Raman measurements were performed. Corresponding Raman spectra are shown below both images. B) Optical micrograph of area where Raman maps were acquired and, to the right, the same image treated with software. Scale bar = 10 μm. Corresponding Raman maps at λ = 514 nm (E_{laser} = 2.41 eV) and λ = 633 nm (E_{laser} = 1.96 eV) are included at the bottom.

particular colored area of interest has been located optically from our transferred samples to SiO₂/Si and has been then re-transferred to a TEM grid. The studied areas by TEM were obtained from yellow- and pink- colored zones. Our TEM observations reveal that the material studied is indeed bi-layer graphene with different rotational angles identified from the diffraction patterns (see the left panels in the **Figures 3A** and **B**) and Fourier transforms of the HRTEM images (not shown here), consequently showing different Moiré patterns in the HRTEM images as seen from the right panels of **Figures 3A** and **B**. The yellow

areas, angles of 11° to 13° correspond to pinkish areas and angles of 13° to 15° correspond to yellowish areas. The above angle assignment matches perfectly our TEM results, where an angle of 12.8° was found for a pink zone and an angle of 13.4° for a yellow zone.

Our observations are validated as well by comparison with results recently published by K. Kim et al.^[24] and R.W. Havener et al.^[27] In the above mentioned reports, the G-band resonance was found for E_{laser} = 1.96 eV at ~10°, such angle of rotation corresponds to a bluish zone where we, as well, found G-band resonance for E_{laser} = 1.96 eV. For E_{laser} = 2.41/2.33 eV their resonance was found at ~13°, corresponding to a pink zone, where we find G band resonance for E_{laser} = 2.41 eV (see **Figure 2**).

We have further confirmed our observations by simulations of the optical contrast of bi-layer graphene using a model that considers the reflection of a system air/bi-layer graphene/SiO₂/Si. Details of the model can be found in the Supporting Information. In order to qualitatively reproduce the effect of the van Hove singularities (vHS) in the optical absorption of tBLG, we have calculated the dielectric function using the graphene refractive index and incorporated a causal Gaussian absorption profile using a Kramers-Kronig analysis. We have estimated the position of the absorption band for each rotation angle by calculating the θ-dependent energy separation of the vHS in tBLG using an empirical formula derived by I. Brihuega et al.^[17]

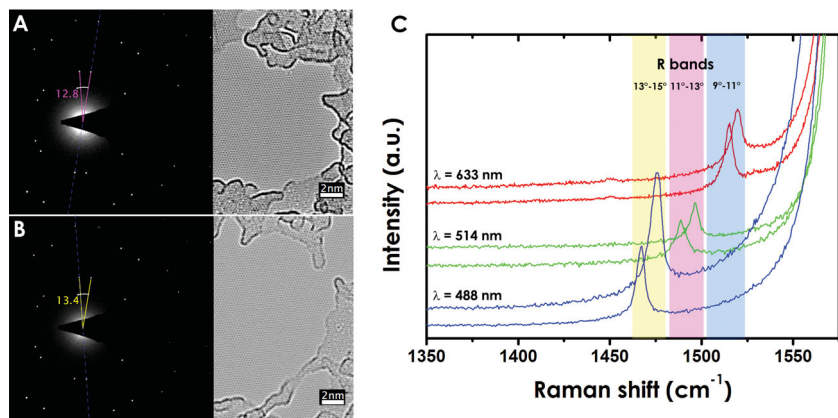


Figure 3. A) and B) left panels, selected-area electron diffraction of pink and yellow colored bi-layer graphene areas; with marked rotation angle between the diffraction spots of 12.8° and 13.4°, respectively. (The values are the averaged value obtained from the diffraction patterns and the Fourier transforms of the HRTEM images (the latter not shown here)). Right panels: corresponding HRTEM images (the image shown is an average over several images). C) Representative Raman spectra of blue, pink and yellow bi-layer graphene areas recorded with λ = 633 nm, λ = 514 nm and λ = 488 nm (red, green and blue curves, respectively). Shaded areas in blue, pink and yellow highlight the frequency regions where R-bands appear for blue-, pink- and yellow- colored tBLG. Corresponding estimated angles are displayed for each color.

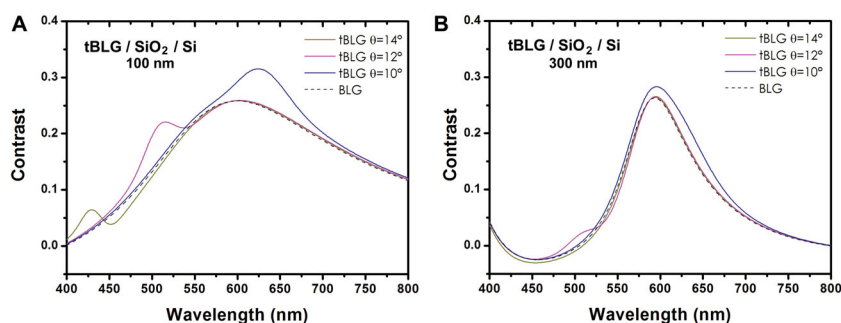


Figure 4. Calculated optical contrast spectra for tBLG/SiO₂/Si systems with different twist angles ($\theta = 10^\circ$, 12° and 14° ; blue, pink and yellow curves, respectively). The SiO₂ thickness was varied in the simulations: A) 100 nm, and B) 300 nm. Black dashed curves represent bi-layer graphene (BLG) for which we have used the monolayer graphene refractive index ($n_g = 2.6 - i1.3$) and twice its thickness.

Using this formula we have been able to derive approximate values for the energy separations of the vHS of tBLG depending on the θ value (ΔE_{vHS}). We have thus estimated the ΔE_{vHS} for 10° , 12° and 14° , which according to our Raman/TEM characterization would correspond to blue, pink and yellow colorations, respectively; consequently we have simulated the absorption of the different tBLG centered on each of these values. We have done these calculations for SiO₂ thicknesses of 100 and 300 nm and plotted the optical contrast of the 3 selected twisted bi-layers. **Figure 4** illustrates the optical contrast of tBLG/SiO₂/Si systems with $\theta = 10^\circ$, 12° and 14° for tBLG (blue, pink and yellow curves, respectively) with different oxide thicknesses: Figure 4A is a simulation for a 100 nm-thick oxide and Figure 4B for 300 nm (the same calculation parameters were used for all the plotted curves).

It is evident that for the oxide layer of 100 nm specific absorption features appear on the spectra of each twisted sample (yellow, pink and blue curves) protruding from the spectrum of bi-layer (black dashed curve). These differences in absorption indicate that the 10° , 12° and 14° tBLG samples will absorb light differently and hence show different colorations, confirming our observations. On the other hand, the same twisted samples on top of a 300 nm-thick oxide layer on Si substrate will only show a slightly pronounced absorption feature for the $\theta = 12^\circ$ twisted sample, while the blue and the yellow curves show a rather similar absorption to that of bi-layer graphene. This is in agreement with our optical observations on 300 nm-thick oxide of mono-tone bi-layer graphene where a slight increase in optical contrast was found for samples resonant with $E_{\text{laser}} = 2.41/2.33$ eV ($\theta = \sim 12^\circ$). The convergence of our simulations proves the validity of our optical microscopy/Raman spectroscopy/HRTEM study.

We have demonstrated using Raman spectroscopy, TEM and theoretical simulations of optical contrast that a spectrum of optical colorations in bi-layer graphene transferred to SiO₂/Si (100 nm oxide thickness) arises from differences in rotational angles between the layers. We have proven that blue-, pink-, and yellow-colored tBLG correspond to areas with mismatch angles of 9° to 11° , 11° to 13° and 13° to 15° , respectively. These results could open new possibilities in technology; the simple optical inspection of bi-layer

graphene samples can yield selective angle-dependent fabrication of devices and thus enable the tunable control of electrical and optical properties.

Experimental Section

Graphene samples were produced by CVD at low pressures with methane as carbon source and copper as catalyst. The produced samples were transferred onto SiO₂/Si (oxide thickness 100 nm) substrates to be able to optically identify single and bi-layer graphene and to perform Raman measurements.

Raman spectroscopy measurements were performed on a LabRam Horiba instrument with

laser excitation energies of 2.54 eV, 2.41 eV and 1.96 eV. Powers have been kept below 1 mW and low and high resolution gratings have been used in our measurements (150 and 1800 g/mm, respectively).

To carry out the TEM studies, the SiO₂/Si transferred samples have been re-transferred to Quantifoil grids via potassium hydroxide.^[31] The sample was annealed at 200 °C for 10 min before introducing into the TEM. HRTEM and selected-area electron diffraction experiments were performed using an aberration-corrected FEI Titan 80–300 operated at 80 kV. The HRTEM images were obtained at Scherzer conditions with a spherical aberration value of 0.02 mm.

Supporting Information

Supporting Information is available from the Wiley Online Library or from the author.

Acknowledgements

JCD thanks A.R. Botello-Méndez, U. Bhaskar and P.A. Haddad for technical assistance and A. Jorio, L.G. Cançado for helpful discussions. JCD acknowledges financial support from CONACyT and FNRS. GAS acknowledges the support from the CONACyT-DAAD stipend and GAS and UK acknowledge the financial support by the DFG and the MWKBW within the SALVE (Sub-Angstrom Low-Voltage Electron Microscopy) Project. JCD and CNS acknowledge the financial support by the ARC project “Stresstronics”. During the proofing of this article, the authors noted that an independent study discussing similar results has appeared recently in the literature.^[32]

- [1] K. S. Novoselov, A. K. Geim, S. V. Morozov, D. Jiang, Y. Zhang, S. V. Dubonos, I. V. Grigorieva, A. A. Firsov, *Science* **2004**, *306*, 666.
- [2] A. C. Ferrari, J. C. Meyer, V. Scardaci, C. Casiraghi, M. Lazzeri, F. Mauri, S. Piscanec, D. Jiang, K. S. Novoselov, S. Roth, A. K. Geim, *Phys. Rev. Lett.* **2006**, *97*, 187401.

- [3] L. M. Malard, J. Nilsson, D. C. Elias, J. C. Brant, F. Plentz, E. S. Alves, A. H. Castro Neto, M. A. Pimenta, *Phys. Rev. B* **2007**, *76*, 201401.
- [4] J. H. Warner, M. H. Rummeli, T. Gemming, B. Büchner, G. A. D. Briggs, *Nano Lett.* **2009**, *9*, 102.
- [5] F. Varchon, P. Mallet, L. Magaud, J.-Y. Veuillen, *Phys. Rev. B* **2008**, *77*, 165415.
- [6] R. Zhao, Y. Zhang, T. Gao, Y. Gao, N. Liu, L. Fu, Z. Liu, *Nano Research* **2011**, *4*, 712.
- [7] P. Poncharal, A. Ayari, T. Michel, J. L. Sauvajol, *Phys. Rev. B* **2008**, *78*, 113407.
- [8] A. Reina, X. Jia, J. Ho, D. Nezich, H. Son, V. Bulovic, M. S. Dresselhaus, J. Kong, *Nano Lett.* **2009**, *9*, 30.
- [9] K. S. Kim, Y. Zhao, H. Jang, S. Y. Lee, J. M. Kim, K. S. Kim, J.-H. Ahn, P. Kim, J.-Y. Choi, B. H. Hong, *Nature* **2009**, *457*, 706.
- [10] X. Li, W. Cai, J. An, S. Kim, J. Nah, D. Yang, R. Piner, A. Velamakanni, I. Jung, E. Tutuc, S. K. Banerjee, L. Colombo, R. S. Ruoff, *Science* **2009**, *324*, 1312.
- [11] Z. H. Ni, W. Chen, Z. F. Fan, J. L. Kuo, T. Yu, A. T. S. Wee, Z. X. Shen, *Phys. Rev. B* **2008**, *77*, 115416.
- [12] J. Hass, F. Varchon, J. E. Millán-Otoya, M. Sprinkle, N. Sharma, W. A. de Heer, C. Berger, P. N. First, L. Magaud, E. H. Conrad, *Phys. Rev. Lett.* **2008**, *100*, 125504.
- [13] R. Bistritzer, A. MacDonald, *Proc. Natl. Acad. Sci. USA* **2011**, *108*, 12233.
- [14] G. Trambly de Laissardière, D. Mayou, L. Magaud, *Phys. Rev. B* **2012**, *86*, 125413.
- [15] G. Li, A. Luican, J. M. B. Lopes dos Santos, A. H. Castro Neto, A. Reina, J. Kong, E. Y. Andrei, *Nat. Physics* **2010**, *6*, 109.
- [16] A. Luican, G. Li, A. Reina, J. Kong, R. R. Nair, K. S. Novoselov, A. K. Geim, E. Y. Andrei, *Phys. Rev. Lett.* **2011**, *106*, 126802.
- [17] I. Brihuega, P. Mallet, H. González-Herrero, G. Trambly de Laissardière, M. M. Ugeda, L. Magaud, J. M. Gómez-Rodríguez, F. Ynduráin, J.-Y. Veuillen, *Phys. Rev. Lett.* **2012**, *109*, 196802.
- [18] W. Yan, M. Liu, R.-F. Dou, L. Meng, L. Feng, Z.-D. Chu, Y. Zhang, Z. Liu, J.-C. Nie, L. He, *Phys. Rev. Lett.* **2012**, *109*, 126801.
- [19] T. Ohta, J. T. Robinson, P. J. Feibelman, A. Bostwick, E. Rotenberg, T. E. Beechem, *Phys. Rev. Lett.* **2012**, *109*, 186807.
- [20] R. R. Nair, P. Blake, A. N. Grigorenko, K. S. Novoselov, T. J. Booth, T. Stauber, N. M. R. Peres, A. K. Geim, *Science* **2008**, *320*, 1308.
- [21] Y. Wang, Z. Ni, L. Liu, Y. Liu, C. Cong, T. Yu, X. Wang, D. Shen, Z. Shen, *ACS Nano* **2010**, *4*, 4074.
- [22] Z. Ni, L. Liu, Y. Wang, Z. Zheng, L.-J. Li, T. Yu, Z. Shen, *Phys. Rev. B* **2009**, *80*, 125404.
- [23] V. Carozo, C. M. Almedia, E. H. M. Ferreira, L. G. Cançado, C. A. Achete, A. Jorio, *Nano Lett.* **2011**, *11*, 4527.
- [24] K. Kim, S. Coh, L. Z. Tan, W. Regan, J. M. Yuk, E. Chatterjee, M. F. Crommie, M. L. Cohen, S. G. Louie, A. Zettl, *Phys. Rev. Lett.* **2012**, *108*, 246103.
- [25] J. D. Wood, S. W. Schmucker, A. S. Lyons, E. Pop, J. W. Lyding, *Nano Lett.* **2011**, *11*, 4547.
- [26] P. Y. Huang, C. S. Ruiz-Vargas, A. M. van der Zande, W. S. Whitney, M. P. Levendorf, J. W. Kevek, S. Garg, J. S. Alden, C. J. Hustedt, Y. Zhu, J. Park, P. L. McEuen, D. A. Muller, *Nature* **2011**, *469*, 389.
- [27] R. Havener, H. Zhuang, L. Brown, R. G. Hennig, J. Park, *Nano Lett.* **2012**, *12*, 3162.
- [28] P. Blake, E. W. Hill, A. H. Castro Neto, K. S. Novoselov, D. Jiang, R. Yang, T. J. Booth, A. K. Geim, *App. Phys. Lett.* **2007**, *91*, 063124.
- [29] D. S. Abergel, A. Russell, V. I. Fal'ko, *App. Phys. Lett.* **2007**, *91*, 063125.
- [30] J. Campos-Delgado, L. G. Cançado, C. A. Achete, A. Jorio, J.-P. Raskin, *Nano Research* **2013**, DOI: 10.1007/s12274-013-0304-z.
- [31] J. C. Meyer, C. O. Meyer, M. F. Crommie, A. Zettl, *Appl. Phys. Lett.* **2008**, *92*, 123110.
- [32] J. T. Robinson, S. W. Schmucker, C. B. Diaconescu, J. P. Long, J. C. Culbertson, T. Ohta, A. L. Friedman, T. E. Beechem, *ACS Nano* **2013**, *7*, 637.

Received: January 6, 2013
Revised: February 20, 2013
Published online: